Bibliography

Lay, T., and Wallace, T. C., 1995. *Modern global seismology.* San Diego: Academic, p. 521.
Reid, H. F., 1910. The mechanism of the earthquake. In *The California Earthquake of April 19, 1906, Report of the State Earthquake Investigation Commission, 2*. Washington, DC: Carnegie Institution, p. 192.
Scholz, C. H., 1990. *The Mechanics of Earthquakes and Faulting*. Cambridge: Cambridge University Press, p. 439.

Cross-references

Earthquake
Earthquake Prediction and Forecasting
Epicenter
Fault
Hypocenter
San Andreas Fault
Seismology

ELECTROMAGNETIC RADIATION (EMR)

Norman Kerle
Faculty of Geo-Information Science and Earth Observation (ITC), University of Twente, Enschede, The Netherlands

Synonyms

Electromagnetic waves; Radiant energy

Definition

Energy propagating through space at the speed of light in the form of sine-shaped electromagnetic waves, composed of perpendicularly arranged electric and magnetic fields. EMR ranges from gamma rays with very short wavelength to long radio waves. The shortest wavelengths can also be modeled as particles (photons). The interaction of EMR with matter forms the basis for remote sensing.

Overview

Electromagnetic radiation (EMR) is composed of sine-shaped waves that propagate through space at the speed of light (approximately 300,000 km s^{-2}), characterized by electrical and magnetic fields that are arranged perpendicular to each other (Lillesand et al., 2004). The central property of EMR is wavelength, inversely proportional to frequency. It ranges from high-frequency gamma rays (with picometer [10^{-16} m] wavelength and that are better thought of as particles or photons) to radio waves many kilometers long and with low frequencies, collectively known as the electromagnetic spectrum (EMS). Wave energy is also proportional to frequency.

EMR forms the basis for remote sensing (RS), which has gained great relevance in studying and monitoring of hazards (Tralli et al., 2005). RS is divided into passive and active methods: reflected or emitted radiation is recorded (passive), or the response of an artificial signal is received (active, for example radar). To detect or monitor phenomena related to hazards, a careful selection of the appropriate part of the EMS is critical. Most Earth observation instruments, such as regular cameras, passively record EMR in the visible part of the spectrum (approximately 0.4–0.7 μm [10^{-6} m]), and in the adjacent near-infrared (NIR, 0.7–1.4 μm). This is ideal to detect the state of vegetation, as the cell structure of healthy green leaves strongly reflects NIR energy, which declines in stressed leaves. Vegetation stress possibly leading to crop failure can thus be detected early.

Less common are detectors that record thermal infrared (TIR) radiation (8–14 μm), for example, to measure surface temperatures. The main forms of active RS are lidar (laser scanning), radar, and sonar (*li*ght/*ra*dio/*so*und *d*etection *a*nd *r*anging, respectively). Lidar uses very short waves between about 400 nm and 1 μm, whereas radar waves range between approximately 0.1–1 m. Sonar uses acoustic waves several meters long. An advantage of all active sensors is that they are largely weather-independent and may also be applied at night.

EMR is also the basis for other tools important in hazard work, for example, GPS, which uses radio waves of about 20 cm, marginally more than other important communication systems, such as wireless networks.

EMR itself can constitute a hazard to living organisms. Well-known examples of radiation to which exposure should be minimized or avoided are X-rays (wavelength of a few nm), ultraviolet rays than cause sunburn (about 0.3–0.4 μm), but also microwaves (wavelength of about 12 cm).

Bibliography

Lillesand, T. M., Kiefer, R. W., and Chipman, J. W., 2004. *Remote Sensing and Image Interpretation*. New York: Wiley.
Tralli, D. M., Blom, R. G., Zlotnicki, V., Donnellan, A., and Evans, D. L., 2005. Satellite remote sensing of earthquake, volcano, flood, landslide and coastal inundation hazards. *ISPRS Journal of Photogrammetry and Remote Sensing*, **59**, 185–198.

Cross-references

Global Positioning System and Natural Hazards
Remote Sensing of Natural Hazards and Disasters

EL NIÑO/SOUTHERN OSCILLATION

Michael Ghil[1,2], Ilya Zaliapin[3]
[1]Ecole Normale Supérieure, Paris, France
[2]University of California, Los Angeles, CA, USA
[3]University of Nevada Reno, Reno, NV, USA

Synonyms

El Niño; Southern oscillation; Tropical pacific warming

Definitions

Easterlies. Low-latitude trade winds that blow from east to west and extend from the Galapagos Islands to Indonesia.
Kelvin wave. A nondispersive subsurface oceanic wave, several centimeters high and hundreds of kilometers wide, that balances the Earth's Coriolis force against the equator.
El Niño. A recurrent increase of the ocean surface temperature across much of the tropical eastern and central Pacific; the term was introduced by Peruvian fishermen.
La Niña. The opposite to El Niño – cooling of the ocean surface temperature across much of the tropical eastern and central Pacific.
Rossby wave. A planetary-scale wave caused by the variation in the Coriolis force with latitude, discovered by Carl-Gustaf Rossby in 1939.
Southern oscillation. Coupled changes in surface air pressure between the eastern and western Pacific associated with El Niño and La Niña events; the term was introduced by Sir Gilbert Walker in 1924.
Southern Oscillation Index (*SOI*). A scalar measure of the strength of Southern Oscillation, calculated as the difference in surface air pressure between Tahiti and Darwin, Australia. El Niño episodes correspond to negative SOI values, La Niñas to positive ones.
Thermocline. A thin layer of ocean water that divides a layer of relatively warm water just below the surface from colder, deeper, nutrient-rich waters. The thermocline is usually a few tens of meters deep in the eastern Tropical Pacific, and can reach depths of hundreds of meters in the western Tropical Pacific. The thermocline depth is heavily affected by El Niño dynamics.
Thermohaline circulation. Large-scale circulation throughout the world's oceans that transforms low-density upper-ocean waters to higher-density intermediate and deep waters, and returns the latter back to the upper ocean.
Walker circulation. Zonal flow in a roughly longitude-altitude plane near the Equator, caused by differences in heat distribution between ocean and land, and described by Sir Gilbert Walker during the 1920s.

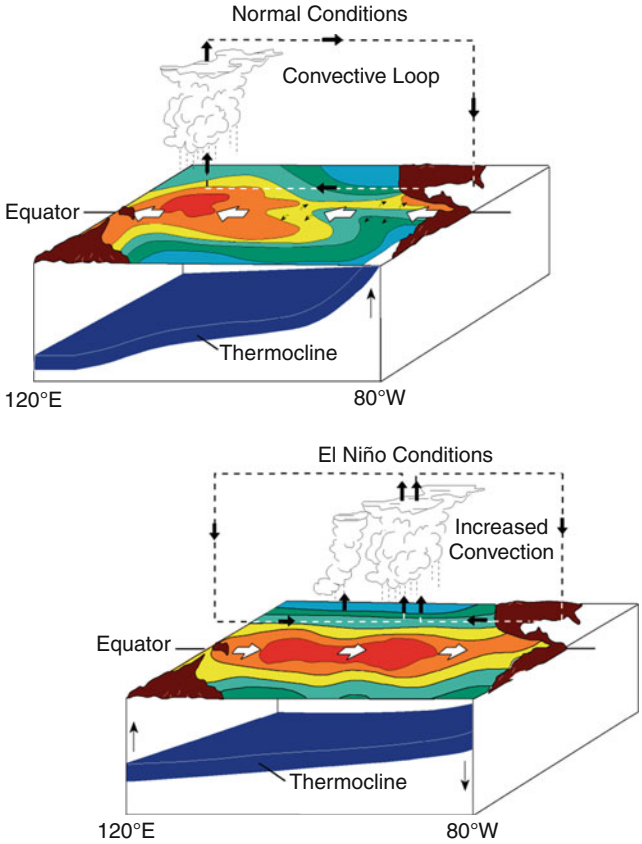

El Niño/Southern Oscillation, Figure 1 Schematic diagram of the atmospheric and oceanic circulation in the Tropical Pacific. *Upper panel*: climatological mean ("normal"), *lower panel*: El Niño (warm) phase. The three-dimensional diagrams show the deepening of the thermocline near the coast of Peru during the warm phase, accompanied by anomalous surface winds (*heavy white arrows*), modified Walker circulation (*lighter black arrows*), and a displacement and broadening of the warmest SSTs from the "warm pool" in the western Tropical Pacific, near Indonesia, toward the east (After McPhaden et al., 1998, with permission of the American Geophysical Union AGU.).

Introduction

The El-Niño/Southern Oscillation(ENSO) phenomenon is the most prominent signal of global seasonal-to-interannual climate variability. It was known for centuries to fishermen and sailors along the west coast of South America, who witnessed a seemingly sporadic and abrupt warming of the cold, nutrient-rich waters that support the food chains in those regions; these warmings caused havoc to the fish harvests (Diaz and Markgraf, 1993; Philander, 1990). The common occurrence of such warmings shortly after Christmas inspired Peruvians to name it El Niño, after the "Christ child" (*el niño* is Spanish for *little boy*). The phenomenon was discussed at the Geographical Society of Lima meeting in 1892, and El Niño became the official name of this phenomenon.

The ENSO phenomenon manifests itself in both atmospheric and oceanic processes (Figure 1). The terms El Niño and La Niña refer to the temperature state of the oceanic surface. An *El Niño* (or warm ENSO phase) represents the warming of waters across much of the tropical eastern and central Pacific. A *La Niña* is the opposite, cooling phase (*la niña* is Spanish for *little girl*). The warm phase occurs typically, to some extent at least, every boreal winter. More significant warm episodes, as well as not so warm ones, occur roughly every 2 years: this is the so-called quasi-biennial oscillation (QBO). In the climate literature, differences between the instantaneous, or short-term average map, and the climatological or *normal* values associated with the mean seasonal cycle are called *anomalies*; in the context of interannual variability, El Niño and La Niña represent, respectively, warm and cold anomalies of sea surface temperature (SST).

These changes in the ocean temperature are directly related to the atmospheric pressure; the changes in pressure between the eastern and western Pacific associated with El Niño and La Niña events are referred to as the *Southern Oscillation*; the term was coined by Sir Gilbert Walker in 1924. El Niño favors higher pressure in the western Pacific; La Niña favors higher pressure in the eastern Pacific.

ENSO dynamics is commonly monitored by averaging SST anomalies over some portion of the Tropical Pacific. The *normal* SST field is defined here in terms of a long-term average (often taken to be 30 years) of mean-monthly maps. There are four regions commonly used for ENSO monitoring:

- Niño 1 + 2 (0°–10°S, 80°–90°W) – the region that typically warms first when an El Niño event develops
- Niño 3 (5°S–5°N; 150°–90°W) – the region with the largest variability in SST on El Niño time scales
- Niño 3.4 (5°S–5°N; 170°–120°W) – the region that is most important for monitoring global climate variability, because the SST variability in this region has the strongest effect on shifting rainfall in the western Pacific and elsewhere
- Niño 4 (5°S–5°N; 160°E–150°W) – the region with average SST close to 27.5°C, which is thought to be an important threshold in producing rainfall

As is typical for threshold-crossing episodes in a continuous field, there is no objective, quantitative definition of ENSO events. Trenberth (1997) addressed the problem of formally defining El Niño and La Niña by suggesting that "an El Niño can be said to occur if 5-month running means of sea surface temperature (SST) anomalies in the Niño 3.4 region exceed 0.4°C for 6 months or more." Table 1 lists all the ENSO events since 1950 according to this definition.

El Niño/Southern Oscillation, Table 1 El Niño and La Niña years, after IRI (2010)

El Niño	Year	La Niña	Year
1	1951	1	1950–1951
2	1953	2	1954–1956
3	1957–1958	3	1964–1965
4	1963–1964	4	1967–1968
5	1965–1966	5	1970–1972
6	1968–1970	6	1973–1976
7	1972–1973	7	1984–1985
8	1976–1977	8	1988–1989
9	1977–1978	9	1995–1996
10	1982–1983	10	1998–2000
11	1986–1988	11	2000–2001
12	1990–1992		
13	1993		
14	1994–1995		
15	1997–1998		

Global climatic and socioeconomic impacts

Starting in the 1970s, El Niño's climatic, and hence socioeconomic, effects were found to be far broader than its manifestations off the shores of Peru (Glantz et al., 1991; Diaz and Markgraf, 1993). This realization was triggered in particular by the strong El Niño episode of 1976–1977 that coincided with a so-called global "climate shift" (Miller et al., 1994) in the Pacific Ocean, and it led to a global awareness of ENSO's significance and to an increased interest in modeling (Cane and Zebiak, 1985; Philander, 1990; Neelin et al., 1992, 1994, 1998), as well as in monitoring and forecasting (Barnston et al., 1994; Latif et al., 1994; Ghil and Jiang, 1998) exceptionally strong El Niño and La Niña events.

Affected by numerous competing mechanisms, the remote effects of ENSO, also called *teleconnections*, do vary from one El Niño or La Niña event to another. Nevertheless, it has been observed that significant ENSO events are consistently related to particular weather anomalies around the globe. In many regions, these anomalies present the second largest contribution to climate variability after the seasonal cycle (IRI, 2010). Seasonal climate changes, in turn, affect the flood and landslide frequencies, air quality, forest fire likelihood, agricultural production, disease outbreaks, fisheries catches, energy demand and supply, as well as food and water availability. Accordingly, both damages and benefits of ENSO's impact present an important component of the socioeconomical and political life of the affected regions. This impact is generally more severe in developing countries, where people's lives are heavily dependent on agricultural production and natural water sources. ENSO effects, as well as any other climate impacts, can be amplified or reduced by such factors as government policies; infrastructure resilience; crop and human diseases; current military, economic, or political conflicts; disruption of storage and shipping facilities; mitigation policies for natural hazards; and many others (IRI, 2010).

In the physical climate system, ENSO affects SSTs, wind, pressure, and rainfall patterns: it does so directly in the Tropical Pacific and via teleconnections in many other parts of the globe. The key observation in understanding ENSO climatic patterns is that the SST field plays a key role in determining rainfall intensity: the higher the SSTs, the higher are the rainfalls. Under *normal conditions* (absence of El Niño), the largest SSTs and greatest rainfall intensity is found over the "warm pool" in the western Tropical Pacific, whereas the eastern Tropical Pacific and the west coast of South America enjoy cold, nutrient-rich waters; the prevailing winds are the *easterly* trade winds. *El Niño conditions* shift the highest SSTs and rainfall eastward and weaken the easterlies; *La Niña conditions* shift high SSTs and rainfall farther west, extend the cold waters to the central Pacific, and strengthen the easterlies. ENSO teleconnections manifest the close relationship between the tropical rainfall and prevailing winds on the one hand and the global atmospheric wind patterns on the other.

A large El Niño event affects, within the next year, the temperature and precipitation patterns along both coasts of South America, the Caribbean, the Equatorial Pacific, Southeast Asia, India, Southeast and West Africa, Australia, and both coasts of North America (Ropelewski and Halpert, 1987; New and Jones, 2000). Hurricanes, typhoons, and tropical cyclones are also affected by ENSO, either directly (in the Pacific) or via teleconnections (in the Indian and Atlantic Oceans): the changes may be seen in the frequency of events or in the initial location of these storms (Landsea, 2000).

The most important impact of El Niño events on local hydroclimatic conditions and thus on regional ecology and economics can be seen in floods and landslides caused by high rainfalls in Southern California and Peru, forest fires and air pollution in Indonesia, crop failures and famine due to droughts in southern Africa, as well as in the collapse of Peruvian anchovy fisheries due to the warming of coastal waters. At the same time, ENSO affects in one way or another all continents and diverse sectors of socio-economic systems around the globe. Table 2 illustrates the global ENSO impacts according to the data from the International Research Institute for Climate and Society (IRI, http://portal.iri.columbia.edu).

What causes ENSO?

The following conceptual elements play a determining role in ENSO dynamics.

The Bjerknes hypothesis. Jacob Bjerknes (1897–1975) laid the foundation of modern ENSO research. Bjerknes (1969) suggested a *positive feedback* as a mechanism for the growth of an internal instability that could produce large positive anomalies of SSTs in the eastern Tropical Pacific. Using observations from the International Geophysical Year (1957–1958), he realized that this mechanism must involve air-sea interaction in the tropics. The "chain reaction" starts with an initial warming of SSTs in the "cold tongue" that occupies the eastern part of the equatorial Pacific. This warming causes a weakening of the thermally direct Walker cell circulation; this circulation involves air rising over the warmer SSTs near Indonesia and sinking over the colder SSTs near Peru. As the trade winds blowing from the east weaken and give way to westerly wind anomalies, the ensuing local changes in the ocean circulation encourage further SST increase. Thus the feedback loop is closed and further amplification of the instability is triggered.

El Niño/Southern Oscillation, Table 2 Global impacts of ENSO (according to the IRI data base http://iri.columbia.edu/climate/ENSO/)

Region	Impact
Africa	Changes in land use
Asia	Changes in available water resources; droughts and floods; changes in river discharge; outbreaks of wheat stripe rust disease, cholera, hemorrhagic fever, dengue; interannual variability of ozone; influence on rice production
Australia and the Pacific	Changes in alpine-lake inflow; changes in river discharge; amount of rainfall; outbreaks of encephalitis; availability of banana prawns
Central America and the Caribbean	Floods; changes of a coastal fish assemblage; variations of annual maize yields; coral bleaching; mortality rates
Europe	Agricultural yields; wine production and quality
North America	Variations in the occurrence of wildfires; annual runoff; insect population
South America	Invertebrate behavior; maize, grain production; precipitation and streamflow; river discharge

Delayed oceanic wave adjustments. Compensating for Bjerknes positive feedback is a *negative feedback* in the system that allows a return to colder conditions in the basin's eastern part. During the peak of the cold-tongue warming, called the *warm* or El Niño phase of ENSO, westerly wind anomalies prevail in the central part of the basin. As part of the ocean's adjustment to this atmospheric forcing, a Kelvin wave is set up in the tropical wave guide and carries a warming signal eastward. This signal deepens the eastern-basin thermocline, which separates the warmer, well-mixed surface waters from the colder waters below, and thus contributes to the positive feedback described above. Concurrently, slower Rossby waves propagate westward, and are reflected at the basin's western boundary, giving rise therewith to an eastward-propagating Kelvin wave that has a cooling, thermocline-shoaling effect. Over time, the arrival of this signal erodes the warm event, ultimately causing a switch to a *cold* or La Niña phase.

Seasonal forcing. A growing body of work (Chang et al., 1994; Jin et al., 1994; Tziperman et al., 1994; Ghil and Robertson, 2000) points to resonances between the Pacific basin's intrinsic air-sea oscillator and the annual cycle as a possible cause for the tendency of warm events to peak in boreal winter, as well as for ENSO's intriguing mix of temporal regularities and irregularities. The mechanisms by which this interaction takes place are numerous and intricate and their relative importance is not yet fully understood (Battisti, 1988; Tziperman et al., 1994; Dijkstra, 2005).

Time series that depict ENSO dynamics

An international 10-year (1985–1994) Tropical-Ocean–Global-Atmosphere (TOGA) Program greatly improved the observation (McPhaden et al., 1998), theoretical modeling (Neelin et al., 1994, 1998), and prediction (Latif et al., 1994) of exceptionally strong El Niño events. It has confirmed, in particular, that ENSO's significance extends far beyond the Tropical Pacific, where its causes lie.

An important conclusion of this program was that – in spite of the great complexity of the phenomenon and the

differences between the spatiotemporal characteristics of any particular ENSO cycle and other cycles – the state of the Tropical Pacific's ocean-atmosphere system could be characterized, mainly, by either one of two highly anticorrelated scalar indices. These two indices are an SST index and the Southern Oscillation Index (SOI): they capture the East-West seesaw in SSTs and sea level pressures, respectively.

A typical version of the SST index is the so-called Niño-3.4 index, which summarizes the mean anomalies of the spatially averaged SSTs over the Niño-3.4 region (Trenberth, 1997). The evolution of this index since 1900 is shown in Figure 2: it clearly exhibits some degree of regularity on the one hand as well as numerous features characteristic of a deterministically chaotic system on the other. The regularity manifests itself as the rough superposition of two dominant oscillations, the quasi-biennial (QBO) and quasi-quadrennial (Jiang et al., 1995c; Ghil et al., 2002) mode, by the phase locking of warm events to boreal winter that gives El Niño its name and by a near-symmetry of the local maxima and minima (i.e., of the positive and negative peaks). The lack of regularity has been associated with the presence of a "Devil's staircase," which is discussed in further detail below (Chang et al., 1994; Jin et al., 1994; Tziperman et al., 1994), and may be due to stochastic effects as well (Ghil et al., 2008a).

A hierarchy of climate models

Climate dynamics has emerged as a modern scientific discipline about a half-century ago (Pfeffer, 1960), and it is within this broader framework that ENSO variability should be considered. The climate system is highly complex, its main subsystems have very different characteristic times, and the specific phenomena involved in various climate problems are quite diverse. It is inconceivable, therefore, that a single model could successfully be used to incorporate all the subsystems, capture all the phenomena, and solve all the problems.

Hence the concept of a *hierarchy of models*, from the simple to the complex, had been developed almost four decades ago (Schneider and Dickinson, 1974). Climate models can be divided into *atmospheric*, *oceanic*, and *coupled*. Each group is characterized, in addition, by the model dimension, where the number of dimensions, from zero to three, refers to the number of independent space variables used to describe the model domain, i.e., to physical-space dimensions. Coupled atmosphere-ocean models – from the simplest zero-dimensional (0-D) ones to three-dimensional (3-D), general circulation models (GCMs) – might be better able to model ENSO dynamics than other climatic phenomena, because ENSO is generally thought to operate through atmosphere-ocean coupling.

A fairly well-developed hierarchy of coupled ocean-atmosphere models has been applied to the problem of seasonal-to-interannual variability in the Tropical Pacific ocean, directly related to ENSO dynamics (Neelin et al., 1994). Its most important rungs are, in ascending order: essentially 0-D simple models, like the delay-oscillator model of Suarez and Schopf (1988); essentially 1-D intermediate coupled models (ICMs: Cane and Zebiak, 1985; Jin et al., 1994); essentially 3-D hybrid coupled models, in which an ocean GCM is coupled to a much simpler, diagnostic atmospheric model (Neelin, 1990; Barnett et al., 1993); and fully coupled GCMs (Neelin et al., 1992; Robertson et al., 1995). Hybrid models of this type have also been applied to climate variability for the mid-latitude (Weng and Neelin, 1998) and global (Chen and Ghil, 1996; Wang et al., 1999) coupled system.

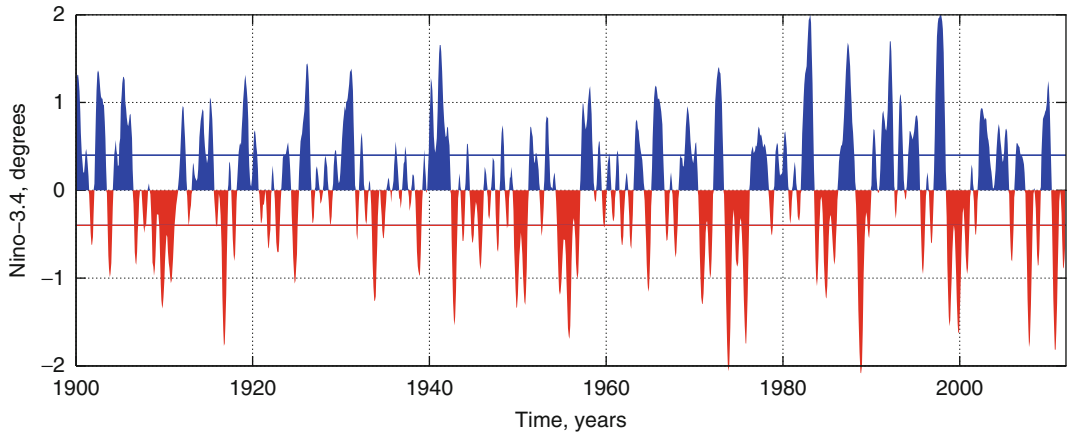

El Niño/Southern Oscillation, Figure 2 Time evolution of the Niño-3.4 index during 1900–2012. The index depicts the sea surface temperature (SST) anomalies (deviations from the climatological mean) in the Niño-3.4 region, between 170°W–120°W and 5°S–5°N. Horizontal lines are drawn at ±0.4°; according to Trenberth (1997), El Niño (warm) and La Niña (cold) events can be defined as a 6-month exceedance of these thresholds.

Modeling ENSO: Goals and approaches

ENSO modeling is focused on a broad twofold goal: (1) to depict the essential mechanisms behind the observed ENSO variability and (2) to forecast future ENSO dynamics, in particular large El Niño and La Niña events that have potential to impact on human activity. The modeling efforts are fostered by understanding the basic physical principles behind the examined phenomenon (see the section above) as well as confronting the existing models with observations.

There are two main paradigms in modeling ENSO variability (Neelin et al., 1994, 1998; Ghil and Robertson, 2000). A *deterministically chaotic, nonlinear* paradigm explains the complexities of ENSO dynamics by the nonlinear interplay of various internal driving mechanisms. For instance, the complex evolution of the SST and thermocline depth can be simulated by the interplay of the two basic ENSO oscillators: an internal, highly nonlinear one, produced by a delayed feedback of the oceanic wave propagation, and a forced, seasonal one (Tziperman et al., 1994; Zaliapin and Ghil, 2010). A *stochastic, linear paradigm*, on the other hand, attempts to explain characteristic features of ENSO dynamics by the action of fast *weather noise* on a linear or weakly nonlinear slow system, composed mainly on the upper ocean near the equator. Boulanger et al. (2004) and Lengaigne et al. (2004), among others, provide a comprehensive discussion of how weather noise could be responsible for the complex dynamics of ENSO, and, in particular, whether westerly wind bursts trigger El Niño events. It seems that any successful modeling effort should combine these two paradigms to obtain richer and more complete insights into climate dynamics in general (e.g., Ghil et al., 2008a).

Much of our theoretical understanding of ENSO comes from relatively simple, essentially 0-D and 1-D coupled models, consisting of a shallow-water or two-layer ocean model coupled to steady-state, shallow-water-like atmospheric models with heavily parameterized physics; the more complete ones among these models are the previously mentioned ICMs (Neelin et al., 1994). In these models, ENSO-like variability results from an oscillatory instability of the coupled ocean-atmosphere's annual-mean climatological state. Its nature has been investigated in terms of the dependence on fundamental parameters, such as the coupling strength, oceanic adjustment time scale, and the strength of surface currents (Jin and Neelin, 1993).

The growth mechanism of ENSO is fairly well established, arising from positive atmospheric feedbacks on equatorial SST anomalies via the surface wind stress, as first hypothesized by Bjerknes (1969). The cyclic nature of the unstable mode is subtler and depends on the time scales of response within the ocean. The next section reviews the deterministic, nonlinear paradigm in understanding ENSO's quasi-periodic behavior; the section emphasizes a toy-modeling approach, which is sufficient to capture the main ENSO-driving mechanisms and, unlike GCMs, can be reviewed here in sufficient detail.

ENSO as a coupled oscillator

The 1980s and 1990s saw the development of a dynamical theory that explains ENSO variability via the interaction of two oscillators: *internal*, driven by the negative feedback associated with oceanic wave propagation, and *external*, due to the seasonal cycle.

Schopf and Suarez (1988), Battisti (1988), Suarez and Schopf (1988), and Battisti and Hirst (1989) demonstrated that ENSO's complex dynamics can be studied using the formalism of *delayed differential equations* (DDE). The first attempts dealt with autonomous DDEs, without seasonal forcing, and with a linear delayed part:

$$\frac{dT}{dt} = -\alpha T(t-\tau) + T \tag{1}$$

Here, T represents the SSTs averaged over the eastern equatorial Pacific. The first term on the right-hand side of Equation 1 mimics the negative feedback due to the Kelvin and Rossby waves, while the second term reflects Bjerknes's positive feedback.

The delay equation idea happens to be very successful in explaining the recurrent nature of ENSO events in easily intelligible mathematical settings. Indeed, the delayed negative feedback does not let a solution of Eq. 1 converge to zero or go to infinity as it would go in the ordinary differential equation case with $\tau = 0$: the delay effect thus creates an internal oscillator whose period depends on the delay and the particular form of the equation's right-hand side. Thus, a simple DDE like Eq. 1 has reproduced some of the main features of a fully nonlinear, coupled atmosphere-ocean model of ENSO dynamics in the tropics (Zebiak and Cane, 1987; Battisti, 1988; Battisti and Hirst, 1989). DDE modeling has also emphasized the importance of nonlinear interactions in shaping the complex dynamics of the ENSO cycle.

At the same time, many important details of ENSO variability still had to be explained. First, a delayed oscillator similar to Eq. 1 typically has periodic solutions with a well-defined period of about 4τ. However, the occurrence of ENSO events is irregular. Second, the period suggested by delay equations deviates significantly from the actual recurrence time of warm events, which is about 2–7 years. The delay τ, which is the sum of the basin-transit times of the westward Rossby and eastward Kelvin waves, can be roughly estimated to lie in the range of 6–8 months. Accordingly, model (1) suggests a period of 24–32 months, at most, for the repeating warm events; this period lies at the lower end of the range of recurrence times. Finally, El Niño and La Niña events always peak during the Northern Hemisphere (boreal) winter, hence their name; such phase locking does not exist in a purely internal delayed oscillator.

The next important step in developing ENSO modeling in the DDE framework was made by Tziperman et al. (1994), who demonstrated that the above discrepancies can be removed by considering nonlinear interactions between the internal oscillator and the external periodic forcing by the seasonal cycle. These authors also introduced a more realistic nonlinear coupling between atmosphere and ocean to reflect the fact that the delayed negative feedback saturates as the absolute value of the key dependent variable T increases.

Munnich et al. (1991) made a detailed comparison between cubic and sigmoid nonlinearities in an iterated map model of ENSO. As a result, the sigmoid type of nonlinearity was chosen in Tziperman et al. (1994), resulting in the periodically forced, nonlinear DDE:

$$\frac{dT}{dt} = -\alpha \tanh[\kappa T(t-\tau_1)] + \beta \tanh[\kappa T(t-\tau_2)] + \gamma \cos(\omega t) \quad (2)$$

Here, the first term on the right represents the westward-traveling Rossby wave, the second term represents the eastward Kelvin wave, and the last one is a seasonal forcing. The parameters α, β, and γ represent the relative strengths of these three driving forces; τ_1 and τ_2 are Rossby and Kelvin wave delays, respectively; ω determines the period of the seasonal forcing; and κ represents the strength of the atmosphere-ocean coupling.

Depending on the parameter values, this model has solutions that possess an integer period, are quasi-periodic, or exhibit chaotic behavior. The increase of solution complexity – from period one, to integer but higher period, and on to quasi-periodicity and chaos – is caused by the increase of the atmosphere-ocean coupling parameter κ. Tziperman et al. (1994) also demonstrated that this forced DDE system exhibits period locking, when the external "explicit" oscillator wins the competition with the internal delayed one, causing the system to stick to an integer period; dependence of the system's period on model parameters is realized in the form of a *Devil's staircase* (see below).

These and other ENSO studies with DDE models have been limited to (1) the linear stability analysis of steady-state solutions, which are not typical in forced systems; (2) case studies of particular trajectories; or (3) one-dimensional scenarios of transition to chaos, where one varies a single parameter, while the others are kept fixed. A major obstacle for the complete bifurcation and sensitivity analysis of such DDE models lies in the complex nature of DDEs, whose numerical and analytical treatment is harder than that of models with no delays.

Zaliapin and Ghil (2010) took several steps toward a comprehensive analysis, numerical as well as theoretical, of DDE models relevant for ENSO phenomenology. These authors considered a simplified version of Eq. 2:

$$\frac{dT}{dt} = -\tanh[\kappa T(t-\tau)] + b\cos(2\pi t) \quad (3)$$

and, for the first time, performed its analysis in the complete 3-D space of the physically relevant parameters: strength of seasonal forcing b, ocean-atmosphere coupling κ, and transit time τ of oceanic waves across the Tropical Pacific. This model reproduces many scenarios relevant to ENSO phenomenology, including prototypes of El Niño and La Niña events; intraseasonal activity reminiscent of Madden-Julian oscillations (Madden and Julian, 1994) or westerly wind bursts; and spontaneous interdecadal oscillations.

The model also provided a good justification for the observed QBO in Tropical Pacific SSTs and trade winds (Philander, 1990; Diaz and Markgraf, 1993; Jiang et al., 1995b; Ghil et al., 2002), with the 2–3-year period arising naturally as the correct multiple (four times) of the sum of the basin transit times of Kelvin and Rossby waves. Zaliapin and Ghil (2010) found regions of stable and unstable solution behavior in the model's parameter space; these regions have a complex and possibly fractal distribution of solution properties. The local continuous dependence theorem (Zaliapin and Ghil, 2010) suggests that the complex discontinuity patterns indicate the presence of a rich family of unstable solutions that point, in turn, to a complicated attractor.

The simple DDE model (3), with a single delay, does reproduce the Devil's staircase scenario documented in other ENSO models, including ICMs and GCMs, as well as in observations (Jin et al., 1994; Tziperman et al., 1994; Ghil and Robertson, 2000). The latter result suggests that interdecadal variability in the extratropical, thermohaline circulation (Dijkstra, 2005; Dijkstra and Ghil, 2005) might interfere constructively with ENSO's intrinsic variability on this time scale. Zaliapin and Ghil (2010) found that model (3) is characterized by *phase locking* of the solutions' local extrema to the seasonal cycle; in particular, solution maxima – i.e., model El Niños – tend to occur in boreal winter. These authors also found multiple solutions coexisting for physically relevant values of the model parameters.

Figure 3 illustrates the model's sensitive dependence on parameters in a region that corresponds roughly to actual ENSO dynamics. The figure shows the behavior of the period P of model solutions as a function of two parameters: the propagation period τ of oceanic waves across the Tropical Pacific and the amplitude b of the seasonal forcing; for aperiodic solutions one takes $P = 0$. Although the model is sensitive to each of its three parameters (b,κ,τ), sharp variations in P are mainly associated with changing the delay τ, which is plotted on the ordinate. This sensitivity is an important qualitative conclusion since in reality the propagation times of Rossby and Kelvin waves are affected by numerous phenomena that are not related directly to ENSO dynamics. The sensitive dependence of the period on the model's parameters is consistent with the irregularity of occurrence of strong El Niños, and can help explain the difficulty in predicting them (Latif et al., 1994; Ghil and Jiang, 1998).

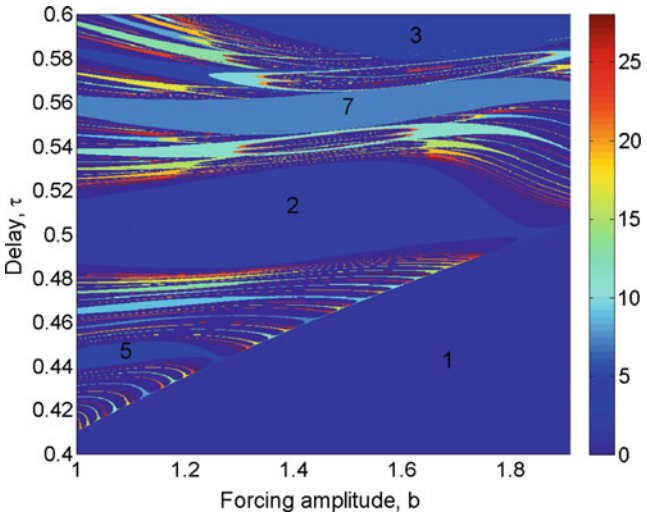

El Niño/Southern Oscillation, Figure 3 Period map for the delayed coupled oscillator of Eq. 3. The figure shows the period P as a function of two model parameters: amplitude b of seasonal forcing and delay τ of the oceanic waves; the ocean-atmosphere coupling strength is fixed at $\kappa = 10$. Aperiodic solutions correspond to $P = 0$. *Numbers* indicate the period values within the largest constant-period regions.

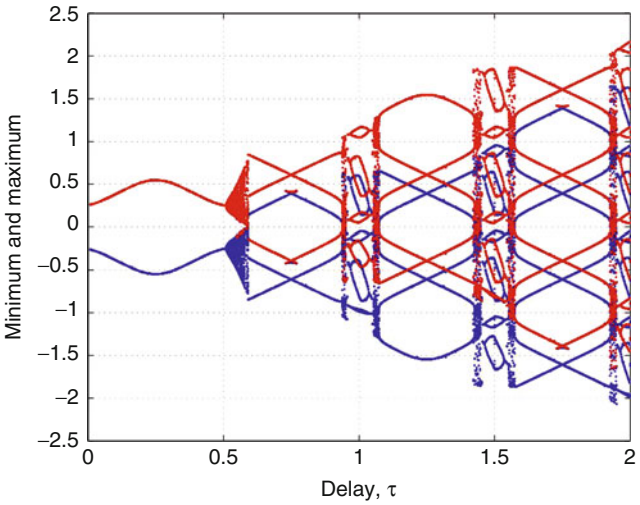

El Niño/Southern Oscillation, Figure 4 Local maxima (*red*) and minima (*blue*) of solutions of Eq. 3 as a function of delay τ; the other parameter values are fixed at $\kappa = 11$ and $b = 2$. Note the aperiodic regimes between periodic windows of gradually increasing period. This figure corresponds to the rightmost vertical section of the region shown in Figure 3 (From Zaliapin and Ghil, 2010).

The model's instabilities disappear and the dynamics of the system becomes purely periodic, with a period of 1 year (not shown), as soon as the atmosphere-ocean coupling κ τ vanishes or the delay τ decreases below a critical value. Figure 4 illustrates this effect in greater detail: the period P of model solutions increases with τ in discrete jumps, $P = 2k + 1$, $k = 0, 1, 2, \ldots$, separated by narrow, apparently chaotic "windows" in τ. This increase in P is associated with the increase of the number of distinct local extrema, all of which tend to occur at the same position within the seasonal cycle. This resembles in fact the behavior of chaotic dynamical systems in discrete time (Kadanoff, 1983) and suggests that the model's aperiodic dynamics is in fact chaotic. This chaotic behavior implies, in particular, that small perturbations in the model parameters or in initial states may lead to significant changes of the model dynamics. Due to this sensitive dependence, forecasting the model's behavior, as well as that of the related natural phenomenon, is a hard problem.

The boundary between the domains of stable and unstable model behavior is clearly visible at the lower right of Figure 3. The period-1 region below and to the right of this boundary contains simple solutions that change smoothly with the values of model parameters. The region above and to the left is characterized by sensitive dependence on parameters. The range of parameters that corresponds to present-day ENSO dynamics lies on the border between the model's stable and unstable regions. Hence, if the dynamical phenomena found in the model have any relation to reality, Tropical Pacific SSTs and other fields that are highly correlated with them, inside and outside the Tropics, can be expected to behave in an intrinsically unstable manner; they could, in particular, change quite drastically with global warming.

Quasi-periodic behavior

The ENSO phenomenon dominates interannual climate variability over the Tropical Pacific. Figure 5, top panel, shows the power spectrum of the monthly SSTs averaged over the eastern equatorial Pacific's Niño-3 area, for the time interval 1960–1997 (Ghil and Robertson, 2000). The observed SST time series contains a sharp annual cycle, together with two broader interannual peaks centered at periods of 44 months (the so-called quasi-quadrennial or low-frequency ENSO cycle) and 28 months (the QBO cycle).

This power spectrum provides a fine example of the distinction between the sharp lines produced by purely periodic forcing and the broader peaks resulting from internal climate variability or from the interaction of the latter with the former. The sharp annual peak reflects the seasonal cycle of heat influx into the tropical Pacific and the phase locking of warm events to boreal winter that gives El Niño its name. The two interannual peaks correspond to the quasi-quadrennial and QBO components of ENSO, as identified by a number of authors (Rasmusson et al., 1990; Allen and Robertson, 1996). These components play a determining role in the ENSO dynamics: Jiang et al. (1995b) have demonstrated that these two

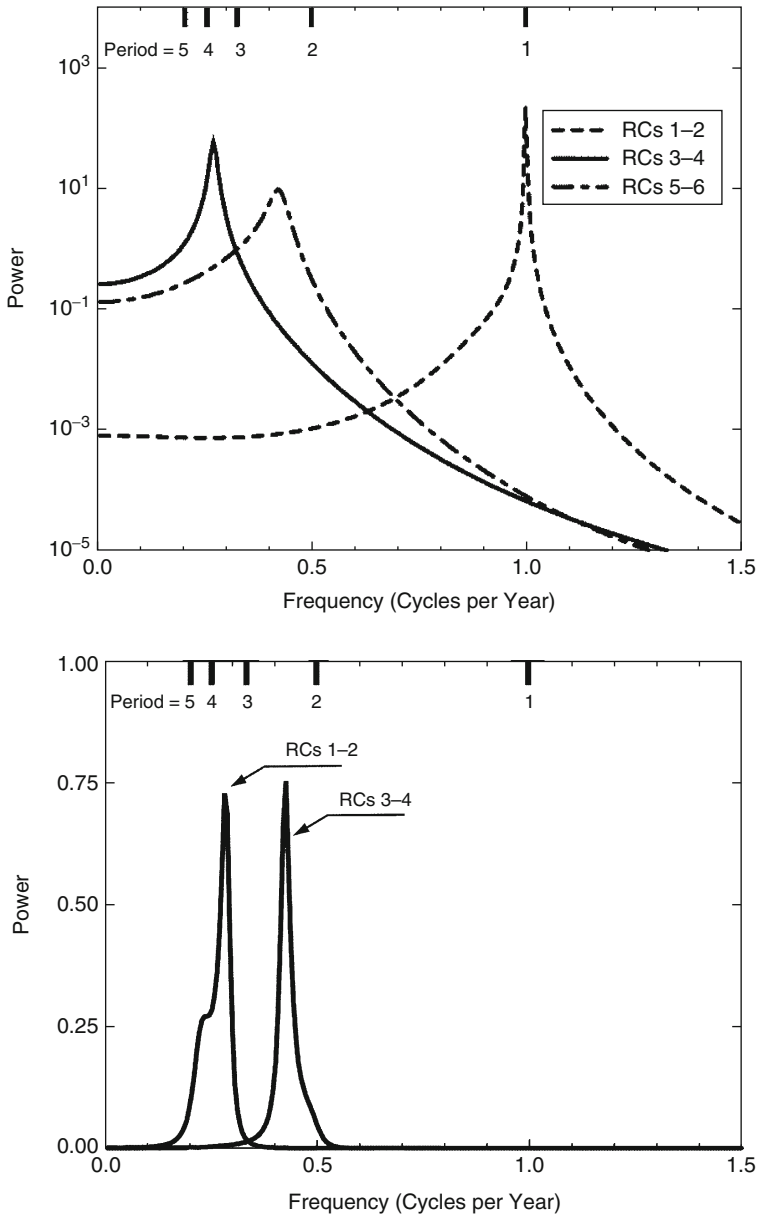

El Niño/Southern Oscillation, Figure 5 *Top*: Power spectrum of the leading reconstructed components (RCs) of the Niño-3 SSTs for the time interval 1960–1997, using monthly data from the Climate Prediction Center of the National Centers for Environmental Prediction (NCEP). An SSA analysis with a window width of 72 months was used to derive the RCs, whose power spectra were then computed using the maximum entropy method, with 20 poles. RCs (1,2) capture the annual cycle, RCs (3,4) the quasi-quadrennial oscillation, and RCs (5,6) the QBO. *Bottom*: Power spectrum of Niño-3 SST anomalies from a 60-year integration of NCEP's coupled GCM, with the seasonal cycle removed (Ji et al., 1998).

components account for about 30% of the variance in the time series analyzed in Figure 5; accordingly, the major El Niño (warm) and La Niña (cold) events during the time interval 1950–1990 can be well reconstructed from ENSO's quasi-quadrennial and QBO components.

The existence of both these oscillatory components has been established in coupled GCMs. The University of California Los Angeles (UCLA) atmospheric GCM, coupled to a tropical-Pacific basin version of the Geophysical Fluid Dynamics Laboratory (GFDL) ocean GCM (Mechoso et al., 2000), is characterized by ENSO-like quasi-quadrennial and QBO modes, but with weaker variability than that of the observed modes (Robertson et al., 1995). A 100-year-long simulation with NASA Goddard's Aries-Poseidon coupled GCM exhibits both quasi-quadrennial and QBO spectral peaks of a strength

very similar to that in observations (not shown). These results are further confirmed by a 60-year run of National Center for Environmental Prediction's (NCEP) coupled GCM (Ji et al., 1998).

Devil's staircase

Various toy and intermediate models (Chang et al., 1994; Jin et al., 1994; Tziperman et al., 1994; Ghil et al., 2008b) have demonstrated that annual forcing causes the internal ENSO cycle to lock to rational multiples of the annual frequency in a Devil's staircase. The period map for the DDE ENSO model of Eq. 3, as shown in Figure 3, is a representative example of this behavior. The Devil's staircase is a function that exhibits peculiar properties, which challenge our intuition about the concept of continuity: it is continuous on the interval [0, 1]; its values span the entire range between 0 and 1; and at the same time it is constant almost everywhere. In other words, the total length of the point sets over which the function increases equals zero!

A classical example of a Devil's staircase, related to the celebrated Cantor set, is shown in Figure 6. Despite its seemingly unnatural features, this type of behavior is commonly seen in coupled, oscillatory mechanical systems, as well as in phase-locked electronic loops (Rasband, 1990). In these systems, the Devil's staircase depicts the relations between the phase of a driven nonlinear oscillatory system and the phase of the external driving force. This staircase represents a generic scenario of transition to deterministic chaos via a subharmonic resonance (e.g., period doubling). Such a scenario involves two parameters: the phase of the external force and the degree of coupling to the driving force.

The period staircase of ENSO also involves two parameters: one governs the period of the intrinsic ENSO instability (i.e., the propagation time of oceanic Kelvin and Rossby waves), whereas the other is the coupling strength between the model's ocean and atmosphere. As the intrinsic period increases, a subharmonic resonance causes frequency locking to successively longer rational multiples of the annual cycle. As the coupling strength increases, the steps on the staircase broaden and begin to overlap, and the model's ENSO cycle becomes irregular, due to jumps between the steps.

The complete Devil's staircase scenario, in fact, calls for successively smaller peaks associated with the harmonics of the 4-year (quasi-quadrennial) mode, at 4/1 = 4, 4/2 = 2, and 4/3 years. Both the QBO and the 4/3-year = 16-month peak are present in observed SST data (Jiang et al., 1995b; Allen and Robertson, 1996). There is a smaller and broader 18–20 month peak present in the UCLA coupled GCM, which can be interpreted as a merged version of these two peaks (Robertson et al., 1995).

Thus, the results of GCM simulations, along with existing observational data, provide reasonable support to the following conjecture: the interaction of the seasonal cycle and the fundamental ENSO mode nonlinearly entrain this mode to a rational multiple of the annual frequency, and produce additional peaks, according to a Devil's staircase. Still, it is possible that different frequency peaks, in particular the quasi-quadrennial and the QBO peaks, could represent separate oscillations, generated by different mechanisms, each with an independent frequency (see Neelin et al., 1998, and references therein).

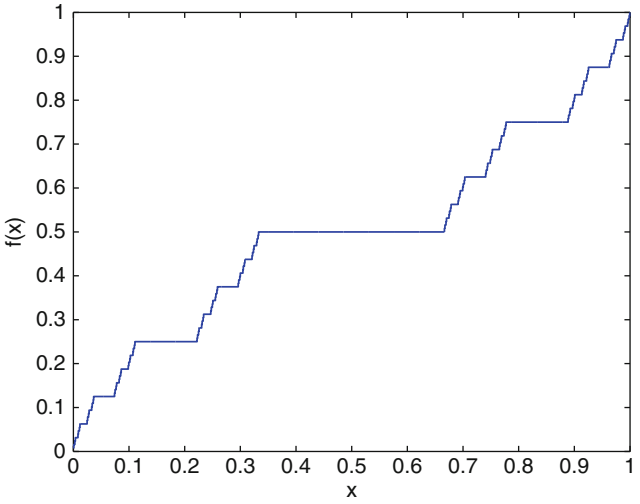

El Niño/Southern Oscillation, Figure 6 Devil's staircase *f(x)*: a continuous function that takes all the values between 0 and 1 and at the same time is constant almost everywhere. There is solid evidence that period locking phenomena in the ENSO system are organized according to a Devil's staircase.

Forecasts

Forecasts of ENSO dynamics are commonly based on modeling and monitoring the evolution of the equatorial Pacific SST. There are two main types of such models: *dynamical* and *statistical*. Roughly speaking, a dynamical model extrapolates the current oceanic and atmospheric conditions into the future by using deterministic principles of atmosphere-ocean interaction. A statistical model uses the past observations to identify conditions that statistically favor occurrence of an El Niño or a La Niña event. The dynamical and statistical models can span the entire modeling hierarchy: from toy to intermediate to fully coupled.

ENSO forecasts are facilitated by (1) the dominant ENSO regularities, mainly the quasi-quadrennial and QBO modes described above, and (2) the persistent nature of ENSO warm and cold episodes, each of which lasts for a few months up to a year. Hence, episode initiation in April–May does facilitate forecasting an event's peak in December–January; likewise, the absence of an episode by June is a very reliable signal for normal conditions in the next year.

In spite of these marked regularities, forecasting El Niño and La Niña events has met with mixed success, even for

short, subannual lead times (Latif et al., 1994). The authors of over a dozen models – all of which routinely produce ENSO forecasts on a monthly or quarterly basis – have noticed year-to-year variations in forecast skill at a lead time of 6–12 months. In addition, forecasts from individual models may significantly vary from one to another.

We illustrate the latter statement with an example of SST forecasts by 15 coupled GCMs (dynamical) and 7 statistical models for the time interval from December 2009 to November 2010, summarized by the International Research Institute for Climate and Society (IRI, 2010); they are shown in Figure 7. All the models start from the observed Niño-3.4 SST anomaly of about 1.8° in December 2009 and try to extrapolate it into the future. Strikingly, this "forecast plume" is characterized by overall regression to the mean of most forecasts: many of the models, dynamical as well as statistical, regress to the no-anomaly mean in about a year. This regression is due to the well-known statistical principle that the best long-term prediction of an ergodic process is its mean. Even so, one observes a persistent 2-degree spread in individual forecasts at all lead times, a spread that characterizes the existing "state-of-the-art" uncertainty in the ENSO prediction problem.

Barnston et al. (1994) and Ghil and Jiang (1998) formally assessed the 6-month lead forecast skills of six ENSO models, three dynamical and three statistical. They used the following two measures of the forecast skill: (1) the Pearson correlation r between the monthly forecast and actual SST anomaly values and (2) the root-mean-squared error (RMSE) of the forecast versus actual SST normalized by the variation of the actual values. This assessment, illustrated in Table 3, suggests that different models have comparable forecast skills with $r \approx 0.65$; these skills are of intermediate quality (RMSE ≈ 0.9), and most probably different models will show different local performance under different circumstances.

Summary and outlook

El Niño/Southern Oscillation (ENSO) is a prominent climatic phenomenon that affects Earth's atmosphere and oceans, as well as their interactions, on time scales up to several years and influences the global climate. ENSO creates anomalies in the sea-surface temperature (SST), thermocline depth, and atmospheric pressure across the Tropical Pacific and affects most immediately the waters off Peru, where this phenomenon was noticed centuries ago. ENSO's oceanic manifestations are called El Niño (warmer waters in the eastern Pacific) and La Niña (colder

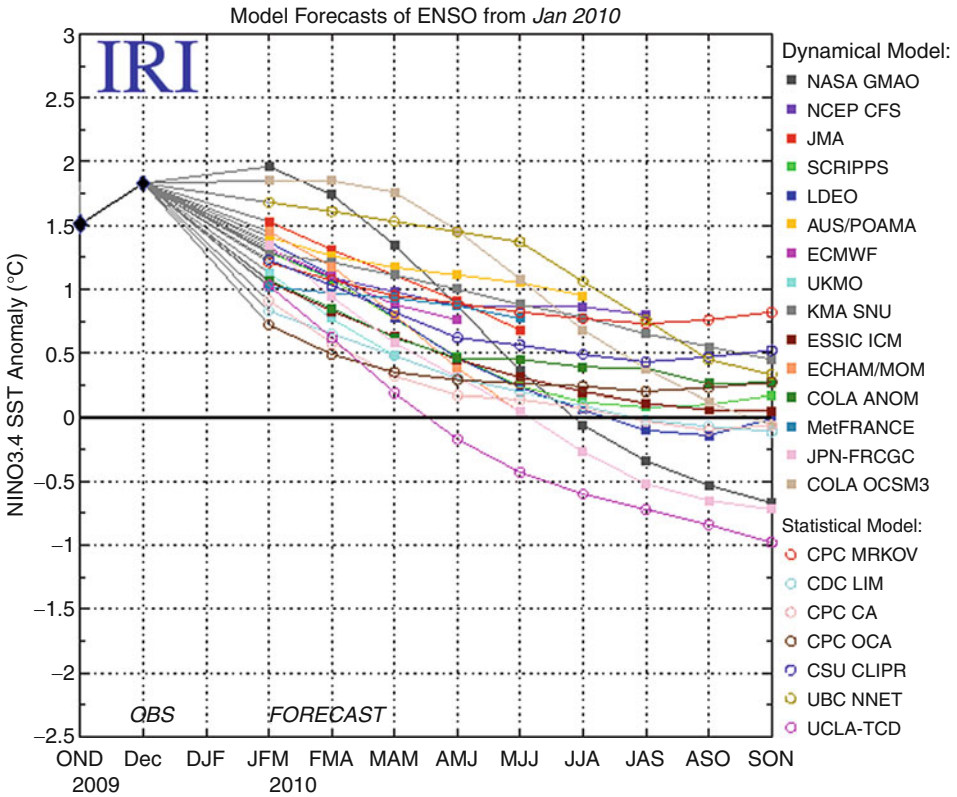

El Niño/Southern Oscillation, Figure 7 "Forecast plume": juxtaposition of SST forecasts for the year 2010, made in December 2009 by 15 dynamical and 7 statistical models (IRI, 2010). Most forecasts regress to the no-anomaly mean within a year, while still giving a persistent 2-degree spread of the individual values at all lead times larger than 3 months.

El Niño/Southern Oscillation, Table 3 Forecast skill (6-month-lead) of six ENSO models (After Ghil and Jiang, 1998, Table 1)

Authors	Zebiak and Cane (1987)	Barnett et al. (1993)	Ji et al. (1994)	Barnston and Ropelewski (1992)	Van den Dool (1994)	Jiang et al. (1995)
Model type	Dynamical			Statistical		
Forecast region	Niño-3	Central Pacific	Niño-3.4			Niño-3
5°S–5°N	90°–150°W	140°–180°W	120°–170°W			90°–150°W
Period	1970–1993	1966–1993	1984–1993	1956–1993	1956–1993	1984–1993
Skill: Correlation	0.62	0.65	0.69	0.66	0.66	0.74
Skill: RMSE	0.95	0.97	0.83	0.89	0.89	0.50

waters there), whereas its atmospheric part is referred to as the Southern Oscillation. The most prominent natural hazards caused by ENSO are felt in all parts of the World (see Table 2); they include local hydroclimatic extremes and affect the regional ecology and economy.

The physical growth mechanism of ENSO is due to the positive atmospheric feedbacks on equatorial SST anomalies via the surface wind stress, cf. Bjerknes (1969). Still, its unstable quasi-periodic behavior prevents robust ENSO predictions, even at subannual lead times. Numerical modeling plays a prominent role in understanding ENSO variability and developing forecasts. There are two main paradigms in ENSO modeling. A *deterministically chaotic, nonlinear* paradigm tries to explain the complexities of ENSO dynamics by the nonlinear interplay of various internal mechanisms. A *stochastic*, *linear paradigm* approaches this problem via the action of fast *weather noise* on an essentially linear, slow system, composed mainly of the upper ocean near the Equator. Despite the existence and importance of comprehensive numerical models, much of our theoretical understanding of ENSO comes from relatively simple models. Initiated in the 1980s, the study of such conceptual models has significantly contributed to shedding new light on many aspects of ENSO, including its quasi-periodic behavior, onset of instabilities, phase locking, power spectrum, and interdecadal variability; some of the most interesting simple models involve delay effects and are summarized herein.

The easiest to forecast are the large-scale SST and sea level patterns in the Tropical Pacific; even here, forecast skill rarely extends beyond 6–12 months. Beyond this ocean basin, atmospheric teleconnections provide some skill in certain parts of the world where ENSO effects are statistically significant, especially during major warm or cold events. Enhanced probabilities for local and regional hazards can be inferred from the larger-scale atmospheric anomalies via downscaling, but such probabilistic forecasts are clearly less reliable than the large-scale patterns on which they are based. Due to the importance of the associated natural hazards, considerable effort is invested in improving these forecasts.

Bibliography

Allen, M. R., and Robertson, A. W., 1996. Distinguishing modulated oscillations from coloured noise in multivariate datasets. *Climate Dynamics*, **12**, 775.

Barnett, T. P., Latif, M., Graham, N., Flügel, M., Pazan, S., and White, W., 1993. ENSO and ENSO-related predictability. Part I: Prediction of equatorial Pacific sea surface temperature with a hybrid coupled ocean-atmosphere model. *Journal of Climate*, **6**, 1545–1566.

Barnston, A., van den Dool, H., Zebiak, S., et al., 1994. Long-lead seasonal forecasts – Where do we stand? *Bulletin of the American Meteorological Society*, **75**, 2097.

Barnston, A. G., and Ropelewski, C. F., 1992. Prediction of NESO episodes using canonical correlation analysis. *Journal of Climate*, **5**, 1316.

Battisti, D. S., 1988. The dynamics and thermodynamics of a warming event in a coupled tropical atmosphere/ocean model. *Journal of the Atmospheric Sciences*, **45**, 2889.

Battisti, D. S., and Hirst, A. C., 1989. Interannual variability in a tropical atmosphere-ocean model – influence of the basic state, ocean geometry and nonlinearity. *Journal of the Atmospheric Sciences*, **46**, 12, 1687.

Bjerknes, J., 1969. Atmospheric teleconnections from the equatorial Pacific. *Monthly Weather Review*, **97**, 163.

Boulanger, J. P., Menkes, C., and Lengaigne, M., 2004. Role of high- and low-frequency winds and wave reflection in the onset, growth and termination of the 1997-1998 El Nino. *Climate Dynamics*, **22**, 267.

Cane, M., and Zebiak, S. E., 1985. A theory for El Niño and the Southern Oscillation. *Science*, **228**, 1084.

Chang, P., Wang, B., Li, T., and Ji, L., 1994. Interactions between the seasonal cycle and the Southern Oscillation: frequency entrainment and chaos in intermediate coupled ocean-atmosphere model. *Geophysical Research Letters*, **21**, 2817.

Chen, F., and Ghil, M., 1996. Interdecadal variability in a hybrid coupled ocean-atmosphere model. *Journal of Physical Oceanography*, **26**, 1561.

Diaz, H. F., and Markgraf, V. (eds.), 1993. *El Niño: Historical and Paleoclimatic Aspects of the Southern Oscillation*. New York: Cambridge University Press.

Dijkstra, H. A., 2005. *Nonlinear Physical Oceanography: A Dynamical Systems Approach to the Large Scale Ocean Circulation and El Niño*, 2nd edn. New York: Springer.

Dijkstra, H. A., and Ghil, M., 2005. Low-frequency variability of the ocean circulation: a dynamical systems approach. *Reviews of Geophysics*, **43**, RG3002.

Ghil, M., 2002. Natural climate variability. In Munn, T. (ed.), *Encyclopedia of Global Environmental Change*. Chichester/New York: Wiley, Vol. 1, pp. 544–549.

Ghil, M., and Jiang, N., 1998. Recent forecast skill for the El Niño/Southern Oscillation. *Geophysical Research Letters*, **25**, 171.

Ghil, M., Allen, M. R., Dettinger, M. D., Ide, K., Kondrashov, D., Mann, M. E., Robertson, A. W., Saunders, A., Tian, Y., Varadi, F., and Yiou, P., 2002. Advanced spectral methods for climatic time series. *Reviews of Geophysics*, **40**, 1003.

Ghil, M., Chekroun, M. D., and Simonnet, E., 2008a. Climate dynamics and fluid mechanics: natural variability and related uncertainties. *Physica D*, **237**, 2111.
Ghil, M., and Robertson, A. W., 2000. Solving problems with GCMs: general circulation models and their role in the climate modeling hierarchy. In Randall, D. (ed.), *General Circulation Model Development: Past Present and Future*. San Diego: Academic, pp. 285–325.
Ghil, M., Zaliapin, I., and Coluzzi, B., 2008b. Boolean delay equations: a simple way of looking at complex systems. *Physica D*, **237**, 2967.
Glantz, M. H., Katz, R. W., and Nicholls, N. (eds.), 1991. *Teleconnections Linking Worldwide Climate Anomalies*. New York: Cambridge University Press.
IRI: The International Research Institute for Climate and Society, 2010. Resources on El Niño and La Niña, http://iri.columbia.edu/climate/ENSO/.
Ji, M., Behringer, D. W., and Leetmaa, A., 1998. An improved coupled model for ENSO prediction and implications for ocean initialization, Part II: the coupled model. *Monthly Weather Review*, **126**, 1022.
Jiang, N., Ghil, M., and Neelin, J. D., 1995a. Forecasts of equatorial Pacific SST anomalies by an autoregressive process using similar spectrum analysis. *Experimental Long-Lead Forecast Bulletin (ELLFB)*, **4**, 24. National Meteorological Center, NOAA, U.S. Department of Commerce.
Jiang, S., Jin, F.-F., and Ghil, M., 1995b. Multiple equilibria, periodic, and aperiodic solutions in a wind-driven, doublee-gyre, shallow-water model. *Journal of Physical Oceanography*, **25**, 764.
Jiang, N., Neelin, J. D., and Ghil, M., 1995c. Quasi-quadrennial and quasi-biennial variability in the equatorial Pacific. *Climate Dynamics*, **12**, 101.
Jin, F.-F., and Neelin, J. D., 1993. Modes of interannual tropical ocean-atmosphere interaction – a unified view. Part III: analytical results in fully-coupled cases. *Journal of the Atmospheric Sciences*, **50**, 3523.
Jin, F-f, Neelin, J. D., and Ghil, M., 1994. El Niño on the Devil's Staircase: Annual subharmonic steps to chaos. *Science*, **264**, 70.
Kadanoff, L. P., 1983. Roads to chaos. *Physics Today*, **12**, 46.
Landsea, C. W., 2000. El Niño/Southern Oscillation and the seasonal predictability of tropical cyclones. In Diaz, H. F., and Markgraf, V. (eds.), *El Niño and the Southern Oscillation: Multiscale Variability and Global and Regional Impacts*. Cambridge: Cambridge University Press, pp. 149–181.
Latif, M., Barnett, T. P., Flügel, M., Graham, N. E., Xu, J.-S., and Zebiak, S. E., 1994. A review of ENSO prediction studies. *Climate Dynamics*, **9**, 167.
Lengaigne, M., Guilyardi, E., Boulanger, J. P., et al., 2004. Triggering of El Nino by westerly wind events in a coupled general circulation model. *Climate Dynamics*, **23**, 601.
Madden, R. A., and Julian, P. R., 1994. Observations of the 40–50-day tropical oscillation – a review. *Monthly Weather Review*, **122**, 814.
Mechoso, C. R., Yu, J.-Y., and Arakawa, A., 2000. A coupled GCM pilgrimage: from climate catastrophe to ENSO simulations. In Randall, D. A. (ed.), *General Circulation Model Development: Past, Present and Future: Proceedings of a Symposium in Honor of Professor Akio Arakawa*. New York: Academic Press, p. 539.
McPhaden, M. J., Busalacchi, A. J., Cheney, R., Donguy, J. R., Gage, K. S., Halpern, D., Ji, M., Julian, P., Meyers, G., Mitchum, G. T., Niiler, P. P., Picaut, J., Reynolds, R. W., Smith, N., and Takeuchi, K., 1998. The tropical ocean-global atmosphere observing system: a decade of progress. *Journal of Geophysical Research*, **103**, 14169.
McWilliams, J. C., 1996. Modeling the oceanic general circulation. *Annual Review of Fluid Mechanics*, **28**, 215.
Miller, A. J., et al., 1994. The 1976-77 climate shift of the Pacific Ocean. *Oceanography*, **7**, 21.
Mitchell, J. M., Jr., 1976. An overview of climatic variability and its causal mechanisms. *Quaternary Research*, **6**, 481.
Munnich, M., Cane, M., and Zebiak, S. E., 1991. A study of self-excited oscillations of the tropical ocean-atmosphere system Part II: nonlinear cases. *Journal of the Atmospheric Sciences*, **48**, 1238.
Neelin, J. D., 1990. A hybrid coupled general circulation model for El Niño studies. *Journal of the Atmospheric Sciences*, **47**, 674.
Neelin, J. D., Latif, M., Allaart, M. A. F., Cane, M. A., Cubasch, U., Gates, W. L., Gent, P. R., Ghil, M., Gordon, C., Lau, N. C., Mechoso, C. R., Meehl, G. A., Oberhuber, J. M., Philander, S. G. H., Schopf, P. S., Sperber, K. R., Sterl, A., Tokioka, T., Tribbia, J., and Zebiak, S. E., 1992. Tropical air-sea interaction in general circulation models. *Climate Dynamics*, **7**, 73.
Neelin, J. D., Latif, M., and Jin, F.-F., 1994. Dynamics of coupled ocean-atmosphere models: the tropical problem. *Annual Review of Fluid Mechanics*, **26**, 617.
Neelin, J. D., Battisti, D. S., Hirst, A. C., Jin, F.-F., Wakata, Y., Yamagata, T., and Zebiak, S., 1998. ENSO theory. *Journal of Geophysical Research*, **103**, 14261.
New, M. G., and Jones, P. D., 2000. Representing twentieth-century space-time climate variability Part II: development of a 1901-96 mean monthly grid of terrestrial surface climate. *Journal of Climate*, **13**, 2217.
Pfeffer, R. L. (ed.), 1960. *Dynamics of Climate*. New York: Pergamon Press.
Philander, S. G. H., 1990. *El Niño, La Niña, and the Southern Oscillation*. San Diego: Academic.
Rasband, S. N., 1990. *Chaotic Dynamics of Nonlinear Systems*. New York: Wiley.
Rasmusson, E. M., Wang, X., and Ropelewski, C. F., 1990. The biennial component of ENSO variability. *Journal of Marine Systems*, **1**, 71.
Robertson, A. W., Ma, C.-C., Ghil, M., and Mechoso, R. C., 1995. Simulation of the Tropical-Pacific climate with a coupled ocean-atmosphere general circulation model. Part II: interannual variability. *Journal of Climate*, **8**, 1199.
Ropelewski, C. F., and Halpert, M. S., 1987. Global and regional scale precipitation patterns associated with the El Niño/Southern Oscillation. *Monthly Weather Review*, **115**, 1606.
Schneider, S. H., and Dickinson, R. E., 1974. Climate modeling. *Reviews of Geophysics and Space Physics*, **25**, 447.
Schopf, P. S., and Suarez, M. J., 1988. Vacillations in a coupled ocean-atmosphere model. *Journal of the Atmospheric Sciences*, **45**, 549.
Suarez, M. J., and Schopf, P. S., 1988. A delayed action oscillator for ENSO. *Journal of the Atmospheric Sciences*, **45**, 3283.
Trenberth, K. E., 1997. The definition of El Niño. *Bulletin of the American Meteorological Society*, **78**, 277.
Tziperman, E., Stone, L., Cane, M., and Jarosh, H., 1994. El Niño chaos: overlapping of resonances between the seasonal cycle and the Pacific ocean-atmosphere oscillator. *Science*, **264**, 272.
Van den Dool, H. M., 1994. Searching for analogues, how long must we wait? *Tellus*, **46A**, 314.
Wang, X., Stone, P. H., and Marotzke, J., 1999. Global thermohaline circulation, Part II: sensitivity with interactive atmospheric transports. *Journal of Climate*, **12**, 83.
Weng, W., and Neelin, J. D., 1998. On the role of ocean-atmosphere interaction in midlatitude interdecadal variability. *Geophysical Research Letters*, **25**, 170.
Zaliapin, I., and Ghil, M., 2010. A delay differential model of ENSO variability, Part 2: phase locking, multiple solutions, and dynamics of extrema. *Nonlinear Processes in Geophysics*, **17**, 123–135.
Zebiak, S. E., and Cane, M. A., 1987. A model for El Niño oscillation. *Monthly Weather Review*, **115**, 2262.